

PARAMETRIC EVALUATION OF HEAT RECOVERY IN A RECUPERATIVE HEAT EXCHANGER

D. L. Sousa^a,W. Balmant^a,

^aUniversidade Federal do Paraná
Departamento de Engenharia Mecânica
Centro Politécnico
Bairro Jardim das Américas
CP. 19011, Curitiba, Paraná, Brasil
diegofine@hotmail.com

ABSTRACT

As urban centers grow and environmental regulations become more stringent, the complexity of integral systems within vehicles, aircraft, and other urban essentials escalates. A pivotal response to this challenge involves achieving enhanced energy efficiency and environmental appeal while maintaining cost-effectiveness. In this context, mathematical modeling, coupled with simulation and optimization techniques, emerges as a pivotal tool. This approach yields favorable outcomes with modest initial investments, contrasting with the resource-intensive nature of purely experimental design. Amongst the fundamental components, heat exchangers find widespread use, facilitating thermal exchange between fluids across diverse applications. Consequently, meticulous design and parametric optimization of these devices to attain peak performance and optimal energy efficiency are imperative, aligning with evolving environmental and energy trends. The simulation of such systems operates within an expansive range of operational and geometric parameters. These encompass mass flow rates, line pressures, pipe diameters, and pipe placements. However, excessive parameter combinations can render optimization computationally infeasible, necessitating judicious simplifications. Striking a balance between precision and computational efficiency, reduced-order models present a valuable intermediary solution. These models, situated between low- and high-order methods, offer robust mathematical representations without significant precision compromises. Thus, reduced-order models, which constitute an intermediate approach when compared to low- and high-order methods, can be used as a mathematical modeling tool without a significant loss of precision in the results. The present work presents an optimization and parametric analysis of a recuperative heat exchanger using a reduced-order approach employing the volume element model (VEM) as a discretization method, which is capable of providing accurate results at low costs. computational. The Laws of Conservation of Mass and Energy are applied to volume elements in combination with empirical correlations in order to quantify the quantities of interest, such as the convection heat transfer coefficient and temperature distribution. A parametric analysis was performed in order to observe the behavior of entropy generation in order to find its minimum points. The mass flow of water varied from 0.001 kg/s to 0.0085 kg/s with the mass flow of hot gases and the mass flow rate of gas was held constant in three stages, namely: 0.14 kg/s; 0.2 kg/s; and 0.3 kg/s. The local minimum was obtained for each of the three gas mass flow rate considerations, 8.53 W/K, 8.78 W/K, and 9.20 W/K respectively.

Received: Ago 20, 2023

Reviewed: Sept 02, 2023

Accepted: Sept 03, 2023

Keywords: volume element model; parametric analysis; recuperative heat

NOMENCLATURE

X quality, Dimensionless
V flow velocity, m/s
T temperature, K
R gas specific constant, J/kg.K
Pr Prandtl Number, Dimensionless
n number of rows in tube arrangement, Dimensionless
m number of tubes per row, Dimensionless
L tube length, m
j element of volume under analysis, Dimensionless
D diameter, m
c specific heat, J/kg.Km total mass of the arrangement, kg

A free stream area, m²
 \dot{V} volumetric flow rate, m³/s
 \dot{m} mass flow rate, kg/s
N number of tubes in one unit cell
N_{ec} number of elemental channels
p pressure, N/m²
Pr fluid Prandtl number, v/α
q heat transfer rate, W
Re_{2b} Reynolds number based on smaller ellipses
t time, s
t_f fin thickness, m
t_t tube thickness, m
T average fluid temperature, K

u_1, u_2, u_3 velocity components, m/s
 W array width, m
 x, y, z cartesian coordinates, m
 X, Y, Z dimensionless cartesian coordinates

Greek symbols

α Thermal Diffusivity, m^2/s
 β Area Density, m^2/m^3
 ε Effectiveness, Dimensionless
 Δ Change in some quantity, Dimensionless
 ρ Fluid Density, kg/m^3

Subscripts

Cond Conduction.
 T Tube.
 FE External Fluid.
 FI Internal Fluid.
 a Anterior.
 P Constant Pressure.
 p Posterior.
 AT Tubular Ring.
 IT Inside Tube.
 ISO Insulator.
 eISO External to Insulation.
 iISO Internal to Insulator.
 Sat Saturation.
 ∞ Free Fluid Stream.
 v Constant Volume; Vapor.
 E External
 0 Initial

INTRODUCTION

As days unfold, society finds itself increasingly reliant on electronic devices, drawn by both the comfort they offer and the seamless execution of tasks at the mere touch of a fingertip or the sound of a voice. The present age witnesses a transformative shift – where tablets replace books, laptops supersede traditional print media, and smartphones serve as conduits for social interactions. Yet, this convenience comes at a cost: a surge in electricity consumption and the mounting tide of discarded electronic waste. This trend warrants a closer examination of the delicate balance between the advantages of electronic integration and the environmental toll it exacts.

It is important to emphasize that the increase in energy consumption, as well as the increase in the production of waste, is closely related to the level of economic activity of a society and because of this, it is a reflection of its global behavior, as well as of industrial, commercial activity. and services.

The pursuit of more sustainable avenues for the repurposing and treatment of municipal solid waste (MSW) has rapidly evolved into a global imperative. In response to this pressing need, novel technologies are being seamlessly integrated into existing systems,

strategically aimed at reversing the ominous trajectory of escalating consumption patterns in the forthcoming years. Projections underscore a disconcerting prospect: by 2050, an estimated 3.5 billion tons of urban solid waste will be generated due to surging population growth and urbanization trends (Kaza et al., 2018). This impending scenario necessitates proactive measures encompassing enhanced product reuse strategies, heightened public awareness, and the judicious exploitation of our energy reserves to ensure heightened efficacy and sustainable outcomes.

An intriguing avenue for repurposing discarded materials lies in harnessing their latent energy potential. A notable method of energy reclamation involves tapping into the latent energy reservoir harbored within waste materials, channeling them into forms of electrical energy, heat, and even fuel through waste treatment processes. This transformative procedure, recognized as waste-to-energy (WtE), offers a compelling means to curtail the volume of materials destined for landfills or alternative storage methods. By effecting the conversion of amassed energy within the residual solid waste (RSW), WtE not only averts wastage but also generates alternative energy forms like thermal and electrical energy (Magnaleli et al., 2020).

Several studies are carried out every year in order to better understand the processes and energy conversion in the biomass burning procedure that occurs inside the system (Santos and Ceribeli, 2013), as well as the search for improvement in efficiency and the reduction of pollutant production, as well as the gases that are released in the combustion process.

Given the aforementioned considerations, it becomes evident that a pivotal contemporary challenge revolves around the augmentation of energy production while upholding stringent environmental preservation standards. In this context, the innovation and advancement of apparatus such as heat exchangers, capable of harnessing energy with minimal dissipation, assume paramount significance. Such innovations not only hold the potential to refine industrial processes but also wield a vital role in curbing the emission of polluting gases, thereby fostering a greener and sustainable industrial landscape (Kuruneru et al., 2021).

The pursuit of elevated energy efficiency and the mitigation of both production costs and environmental ramifications necessitates the exploration of intricate systems. Yet, the viability of these endeavors hinges on the expeditious acquisition of insights. In this regard, the practice of modeling and simulation emerges as a potent technique, enabling the meticulous examination and optimization of a spectrum of physical, biological, electrical, thermal, and mechanical elements. This multifaceted approach stands as an indispensable instrument, facilitating the enhancement and refinement of various equipment and devices, thereby propelling progress across diverse domains.

the cultivation of microalgae using flue gases rich in agro-industrial waste diluted in water as a culture medium. The FBR system depicted here consists of six units, each with a capacity of 10 m³ of culture medium.

2. MATHEMATICAL MODELING IN A REDUCED ORDER FOR HEAT EXCHANGERS

The mathematical model presented in this article proposes a reduced-order approach for the heat exchangers (HX1, HX2, and HX3). It is based on the fundamental principles of classical thermodynamics, which encompass the conservation of mass, conservation of energy, and heat transfer concepts. The discretization process involves dividing the system domain into finite centered volumes called volume elements. Unlike methods such as finite differences, finite elements, and finite volumes, the size of each volume element does not need to be small to ensure numerical stability and result accuracy. This section describes the mathematical modeling for the three analyzed heat exchangers and outlines the associated simplifications.

3.1 Mathematical Modeling of Heat Exchangers HX1, HX2 and HX3

Figures 2, 3, and 4 depict the schematic diagrams of the three heat exchangers. In Figure 2, the division of volume elements is shown, but this step will be omitted in the subsequent figures as it follows the same procedure. The mathematical model is derived by applying the principles of conservation of mass and energy to the system.

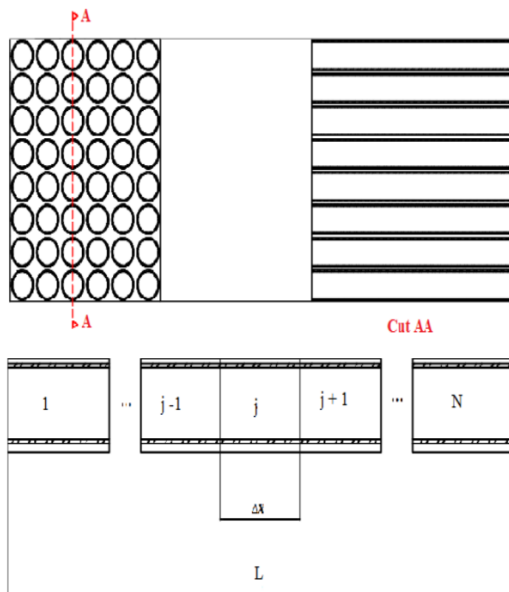


Figure 2. Schematic diagram of recuperative heat exchangers (XH1) and the division of the system into volume elements.

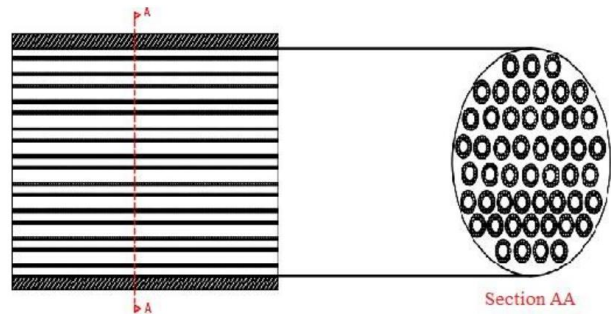


Figure 3. Schematic diagram of recuperative heat exchangers (XH2).

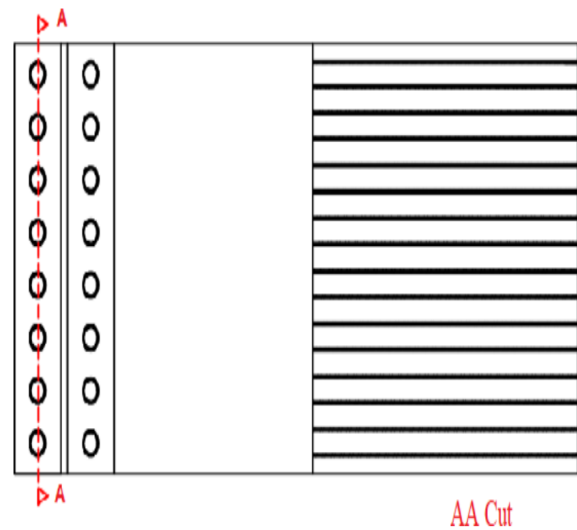


Figure 4. Schematic diagram of recuperative heat exchangers (XH3).

The equipment was initially divided into volume elements, as shown at the bottom of Figure 2. Figure 5 provides further details on the mass and energy transfers within each volume element, revealing a mixed behavior involving both fluid and solid components. To characterize the functionality and performance of each heat exchanger and determine the phase of the fluid (in this case, water) within them (whether it is subcooled, undergoing phase change, or

superheated), each volume element is further divided into five subsystems. These subsystems are as follows:

1. Tube (solid part)
2. Hot gases
3. Subcooled liquid
4. Phase change
5. Superheated steam.

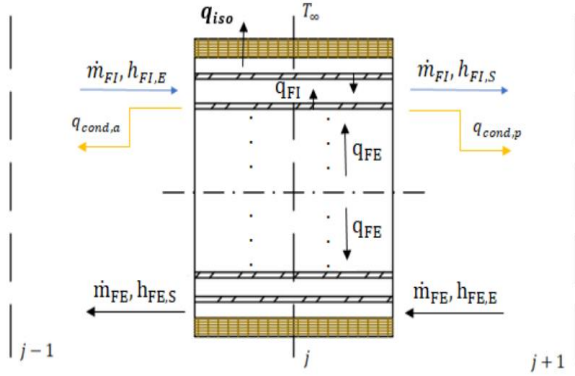


Figure 5. Detail of the volume element, where the mass and heat interactions between subsystems can be observed.

It is important to highlight that each subsystem exists within all three heat exchangers (HX1, HX2, and HX3), but their presence and characteristics may vary across the different exchangers. For instance, HX1 functions as an economizer, utilizing energy from waste combustion gases to heat water to temperatures close to saturation. As a result, subsystems 4 and 5, which pertain to phase change and superheated steam, respectively, are not applicable in HX1 since only liquid is present. The division into subsystems remains essential for all three exchangers as it enables strategic mapping of the phase change point, where the liquid reaches saturation temperature and the vapor fraction (X) starts to vary until reaching unity. The subsequent step involves the mathematical modeling of each subsystem within the volume element, as illustrated in Figure 6. This analysis employs principles of combined mass and energy conservation, as well as the evaluation of energy interactions between subsystems. Equations are employed to quantify these interactions accurately.

Subsystem 1: Tube (solid part): The 1st Law of Thermodynamics is applied to system 1, according to the diagram above, the following equation is obtained:

$$m_{T,j} \cdot c_T \cdot \frac{dT_{T,j}}{dt} = q_{FE,j} + q_{Cond,a,j} + q_{Cond,p,j} - q_{FL,j} \quad (1)$$

Where

$$q_{FE,j} = h_{FE,j} \cdot A_{ET,j} \cdot (T_{FE,j} - T_{T,j}) \quad (2)$$

$$q_{Cond,a,j} = -k_{T,j} \cdot A_{AT,j} \cdot \frac{(T_{T,j} - T_{T,j-1})}{\Delta x} \quad (3)$$

$$q_{Cond,p,j} = -k_{T,j} \cdot A_{AT,j} \cdot \frac{(T_{T,j} - T_{T,j+1})}{\Delta x} \quad (4)$$

$$q_{FL,j} = h_{FL,j} \cdot A_{IT,j} \cdot (T_{T,j} - T_{FL,j}) \quad (5)$$

Where

$$q_{FE,j} = h_{FE,j} \cdot A_{ET,j} \cdot (T_{FE,j} - T_{T,j}) \quad (6)$$

$$q_{Cond,a,j} = -k_{T,j} \cdot A_{AT,j} \cdot \frac{(T_{T,j} - T_{T,j-1})}{\Delta x} \quad (7)$$

$$q_{Cond,p,j} = -k_{T,j} \cdot A_{AT,j} \cdot \frac{(T_{T,j} - T_{T,j+1})}{\Delta x} \quad (8)$$

$$q_{FL,j} = h_{FL,j} \cdot A_{IT,j} \cdot (T_{T,j} - T_{FL,j}) \quad (9)$$

Subsystem 2: Hot gases (external flow): Applying the first law of thermodynamics to subsystem two, which consists of the hot gases that were processed in the incinerator and in the post-combustion chamber, as shown in Figure 6, and assuming variables without a subscript for the hot fluid, we have:

$$m_{FE} c_{v,FE} \frac{dT_{FE,j}}{dt} = \dot{m}_{FE,j} c_{p,FE} (T_{FE,j+1} - T_{FE,j}) - q_{FE,j} - q_{ISO,j} \quad (10)$$

Where

$$q_{ISO,j} = (U \cdot A)_{ISO,j} \cdot (T_{FE,j} - T_{\infty}) \quad (11)$$

$$(U \cdot A)_{ISO,j} = \left[\frac{1}{h_{FE,j} \cdot A_{iISO}} + \frac{\ln\left(\frac{d_{eISO,j}}{d_{iISO,j}}\right)}{2 \cdot \pi \cdot k_{ISO} \cdot L} + \frac{1}{h_{\infty,j} \cdot A_{eISO}} \right] \quad (12)$$

$$A_{eISO} = \pi \cdot d_{eISO,j} \cdot \Delta x \quad (13)$$

$$A_{iISO} = \pi \cdot d_{iISO,j} \cdot \Delta x \quad (14)$$

The boundary conditions are:

$$T_0 = T_E \text{ and } \frac{\partial T}{\partial x} = 0 \quad (15)$$

Subsystem 3: Subcooled liquid: Again the 1st law of thermodynamics is applied to subsystem 3, as seen in Figure 6, providing the following equation:

$$m_{FL,j} \cdot c_{P,FI} \cdot \frac{dT_{FL,j}}{dt} = \dot{m}_{FL,j} \cdot c_{P,FI} \cdot (T_{FL,j-1} - T_{FE,j}) + q_{FL,j} \quad (16)$$

$$q_{FL,j} = h_{FL,j} \cdot A_{FL,j} \cdot (T_{T,j} - T_{FL,j}) \quad (17)$$

Where

$$A_{FL,j} = \pi \cdot \frac{d_{T,j}^2}{4} \quad (18)$$

$$m_{FL,j} = \rho_{FL,j} \cdot \pi \cdot \frac{d_{T,j}^2}{4} \cdot \Delta x \quad (19)$$

The boundary conditions are:

$$T_{r,n} = T_{r,E} \text{ and } \frac{\partial T_{r,o}}{\partial x} = 0 \quad (20)$$

Subsystem 4: Phase change: For the mathematical modeling of the phase change process, a quasi-permanent regime will be considered, that is, the deviations that a given property undergoes in time is considered to be infinitesimal when comparing their changes in space. Thus, applying energy conservation, one has to $\frac{dE}{dt} = 0$ during the integration interval, Δt , which is justified for small amounts of Δx .

$$0 = \dot{m} \cdot X_{j-1} \cdot h_v + \dot{m} \cdot (1 - X_{j-1}) \cdot h_l - \dot{m} \cdot X_j \cdot h_v - \dot{m} \cdot (1 - X_j) \cdot h_l + q_{FL,j} \quad (21)$$

Subsystem 5: Superheated steam: The modeling for subsystem 5 follows the same process as for subsystem 3, however, now the physical properties needed to quantify the quantities will be done for superheated steam.

$$m_{FL,v,j} \cdot c_{v,FI} \cdot \frac{dT_{FL,v,j}}{dt} = q_{FL,v,j} + \dot{m}_{FL,v,j} \cdot c_{P,FI} \cdot (T_{FL,j-1} - T_{FE,j}) \quad (22)$$

In which

$$q_{FL,v,j} = h_{FL,v,j} \cdot A_{FL,j} \cdot (T_{FL,v,j-1} - T_{FL,v,j}) \quad (23)$$

The mathematical model was computationally implemented using MATLAB® (developed by MathWorks Inc.). The objective was to obtain an approximate solution to the system of basic equations mentioned earlier. It is essential to highlight that this set of equations exhibits a mixed characteristic. Specifically, for subsystem 4, operating under nearly steady-state conditions, the resulting equation for each

EV becomes algebraic. To address this, the iterative Gauss-Seidel method was applied, facilitating the approximate solution of these equations.

Furthermore, it is important to note that the heat transfer coefficients for water and hot gases were assumed to be constant. This means that any changes in these coefficients, such as those associated with the phase change of liquid water, were not considered a priori.

The thermodynamic objective function is derived through a careful consideration of entropy generation rate (\dot{S}). The methodology, as proposed by Bejan in 1977, is elucidated by Equation 24, offering insights into the interaction of two counter-current flows based on temperature and pressure variables.

$$\dot{S} = \dot{m}_H \left[c_{P,H} \left(\frac{T_{H,2}}{T_{H,1}} \right) - R_H \left(\frac{P_{H,2}}{P_{H,1}} \right) \right] + \dot{m}_C \left[c_{P,C} \ln \left(\frac{T_{C,2}}{T_{C,1}} \right) - R_C \ln \left(\frac{P_{C,2}}{P_{C,1}} \right) \right] \quad (24)$$

The use of the equation in question arises from the need for a rigorous and comprehensive approach in the analysis of thermodynamic systems. The combination of these two aspects - effectiveness and entropy generation - provides a holistic view of heat exchanges in complex systems. This is particularly relevant in countercurrent flows, where fluid interaction occurs more efficiently compared to concurrent flows. By considering both factors, the equation enables project optimization, bottleneck identification, and informed decision-making to enhance energy efficiency and minimize irreversible losses. Thus, the choice to employ this equation reflects the pursuit of a deeper understanding of the thermodynamic relationships involved in the studied systems. By uniting effectiveness and entropy, the equation offers a valuable tool for engineers and researchers seeking to maximize energy efficiency and sustainability across a range of applications, from heat exchangers to complex industrial processes.

The mathematical model was meticulously translated into a computational framework employing MATLAB® (developed by MathWorks Inc.). This computational endeavor aims to procure an approximate solution for the system of fundamental equations outlined earlier. Notably, it's imperative to recognize the composite nature of this equation set. Particularly, for subsystem 4, characterized by near-perpetual operation, each EV yields an algebraic equation. In navigating this intricacy, the iterative Gauss-Seidel method was judiciously employed, facilitating the derivation of an approximate solution for these equations. Furthermore, a foundational assumption anchors the investigation: the heat transfer coefficients pertinent to both water and hot gases remain steadfast, unswayed by extraneous factors. As

such, changes affecting these coefficients, such as those induced by the phase change of liquid water, remain relegated from consideration in this study.

The equations developed for the other subsystems can be explicitly integrated in relation to time using an adaptive time step with the fourth and fifth order Runge-Kutta method (KINCAID and CHENEY, 1991). The time step is automatically traversed according to the local truncation error, which is kept below a compatible tolerance of 10^{-6} .

RESULTS AND DISCUSSION

The initial conditions used in the simulations were $T_{\infty} = 298.15$ K for $1 \leq j \leq n$. The physical parameters used in this work to simulate the system shown in figures 2, 3, 4 and 5 were $n = 20$ for the converged mesh, the choice of the number of volume elements was made following the work done by Dilay et al. (2014), $L = 2$ m, $\dot{m}_w = 1.01$ kg.s⁻¹, $\dot{m}_g = 3.5$ kg.s⁻¹, $c_{p,g} = 1.004$ kJ.kg⁻¹.K⁻¹, $c_{v,g} = 0.717$ kJ.kg⁻¹.K⁻¹, $h_g = 2.2$ W.m⁻².K, $h_w = 5.1$ W.m⁻².K, $\rho_{w,L} = 1000$ kg/m³, $r_i = 0.5$ m, $r_e = 0.55$ m, $c_{p,sh} = 2$ kJ.kg⁻¹.K⁻¹, $c_{v,sh} = 1.5$ kJ.kg⁻¹.K⁻¹, $P_{sat} = 101325$ Pa, $R_w = 0.46152$ kJ.kg.K, $c_{w,L} = 4.18$ kJ.kg⁻¹.K⁻¹, $\rho_{steel} = 7854$ kg/m³, $c_{steel} = 0.434$ kJ.kg⁻¹.K⁻¹, $\rho_g = 1.225$ kg/m³, $\rho_{w,L} = 1000$ kg/m³, $\rho_{w,vap} = 0.59$ kg/m³, $k_{steel} = 0.036$ kW/m.K, $h_{w,L} = 417.46$ kJ/kg, $h_{w,vap} = 2675.5$ kJ/kg, $u_{w,L} = 417.46$ kJ/kg, $u_{w,vap} = 2675.5$ kJ/kg, $T_{in,air} = 1200$ °C and $T_{sat,w} = 100$ °C.

Figure 6 illustrates the steady-state behavior of the water temperature variation along the flow in the countercurrent heat exchanger as a function of its length.

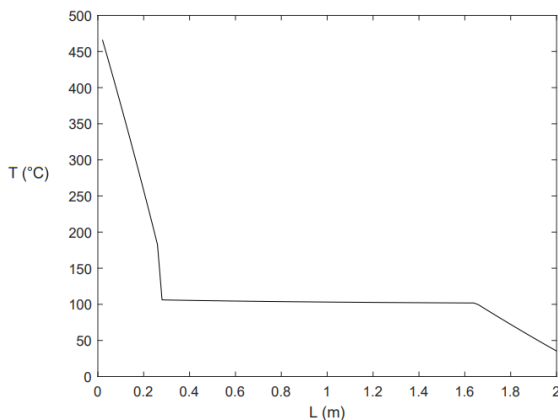


Figure 6. Evolution of water temperature in the heat exchanger for a tube length of 2 m.

The water enters at a temperature of 25 °C and leaves at approximately 416.37 °C as it flows countercurrent to the flow of hot gases along the length of the tube.

Figure 7 illustrates the behavior of the two fluid streams. The dashed line represents the hot gas modeled as air. The solid line represents the water.

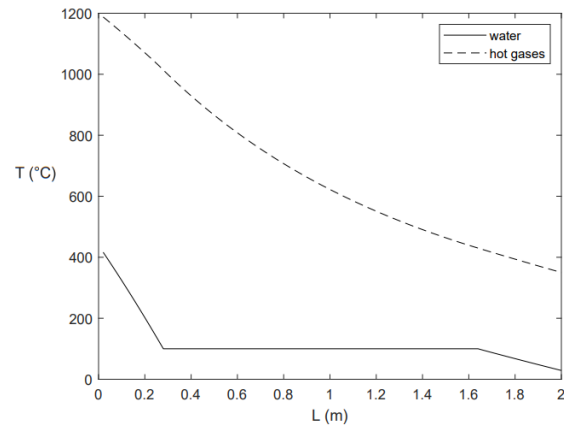
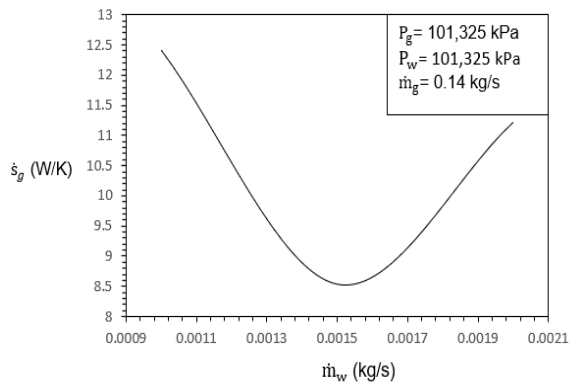


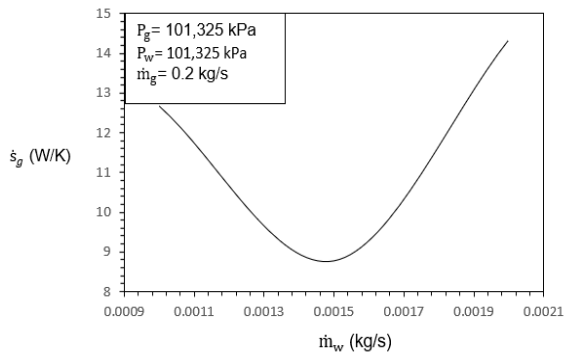
Figure 7. Visualization of fluid streams - hot gas (dashed line) and water (solid line).

The system in question involves a heat transfer process between water and a gas modeled as air through three countercurrent heat exchangers, operating as a boiler: an economizer, a phase change heat exchanger, and a superheater. The economizer serves as the initial heat exchanger. At this stage, water enters at ambient temperature, 25°C, and receives heat energy from the gas, which enters the boiler at a temperature of 1200°C resulting from fuel combustion. This process allows preheating of the feedwater before it enters the phase change heat exchanger, enhancing system efficiency by harnessing the residual heat from the hot gas. Subsequently, the preheated water enters the phase change heat exchanger, where it undergoes a vaporization process. As the water absorbs heat from the hot gas, it undergoes a phase change at constant temperature and pressure, transforming into vapor. This process is crucial for energy generation, as the water vapor is used to drive turbines that generate electricity. Heat transfer in this heat exchanger occurs in countercurrent, maximizing the efficiency of thermal energy transfer. Following the phase change, the saturated vapor is directed to the superheater. In this stage, the vapor is further heated, reaching a temperature of approximately 416.37°C. This temperature increase is vital to ensure that the vapor possesses sufficient thermal energy to efficiently drive the turbines. The hot gas, in turn, continues to transfer heat to the vapor, but its temperature decreases as it loses thermal energy.

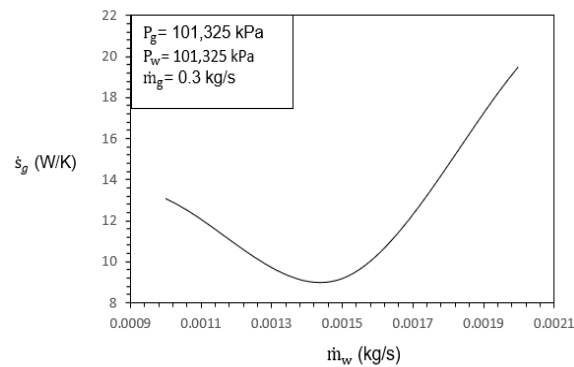
Figure 8 shows the behavior of entropy generation curves as a function of water mass flow for three levels of gas mass flow. In this case, (a) for 0.14 kg/s, (b) for 0.2 kg/s and (c) 0.3 kg/s.



(a)



(b)



(c)

In a countercurrent heat exchanger with flow between water and hot gases, the entropy generation rate increases as we adjust the mass flow rate of water while keeping the gas flow rate constant at three levels, 0.14, 0.2, and 0.3 kg/s. This rise in entropy generation rate is linked to the temperature difference between the fluids and their interaction during the heat exchange process. When the mass flow rate of water is varied, the amount of heat transferred between water and hot gases also varies. If the water flow rate is increased, more heat is transferred, resulting in a decrease in water temperature as it absorbs heat from the gases. This leads to a reduction in the efficiency of heat transfer, as the temperature difference between the fluids decreases. As the temperature difference between the fluids diminishes, the efficiency of heat transfer is compromised, leading to an increase in the

entropy generation rate. Entropy is a measure of the irreversibility of a process, and the less efficient the heat transfer, the greater the amount of energy dissipated irreversibly, contributing to an increase in entropy. Therefore, as we vary the mass flow rate of water while keeping the flow of hot gases constant in a countercurrent heat exchanger, the entropy generation rate increases due to the reduced efficiency of heat transfer caused by the decrease in the temperature difference between the fluids.

CONCLUSIONS

In this study, the Element of Volume Method (VEM) was harnessed to mathematically model an intricate engineering system—a recuperative heat exchanger. This system comprises diverse subsystems, each characterized by its unique attributes. Additionally, these subsystems interact via heat and mass transfer mechanisms. The outcome of our endeavor is the development of a mathematical model tailored for a widely used engineering apparatus: the recuperative heat exchanger. The application of VEM has allowed us to illustrate the evolution of temperatures within this system with remarkable efficiency, employing a modest number of volume elements (VEs), specifically in the case of $n=20$. This judicious choice not only translates to swift simulations but also produces accurate insights into the countercurrent flow of water and hot gas under the assumption of constant heat transfer coefficients.

ACKNOWLEDGEMENTS

I would like to thank the to the Brazilian National Council of Scientific and Technological Development, CNPq (projects 407198/2013-0, 403560/2013-6, 407204/2013-0, 430986/2016-5, 443823/2018-9, 313646/2020-1, 310708/2017-6, 308460/2020-0 and 446787/2020-5), CAPES, Ministry of Education, Brazil (projects 062/14 and CAPES-PRINT-UFPR-88881.311981/2018-01), and Araucaria Foundation of Parana, Brazil (project 115/2018, no. 50.579 – PRONEX).

I would like to express my heartfelt gratitude to my friend, professor, and co-advisor, Wellington Balmant. For all the knowledge, trust, and dedication invested throughout these years. Thank you very much.

REFERENCES

- Bejan A.; Mamut, E. Thermodynamic Optimization of Complex Energy Systems. Neptum, Ramania: Springer, 1998. 465 p. v. 3. ISBN 978-0-7923-5726-1.
- DILAY et al. A volume elemento model (VEM) for energy systems engineering. Rev. International Journal of Energy Research, John Wiley & Sons, v. 39, p. 46-74, 2014.

Kaiser, K. L. Electromagnetic compatibility handbook. CRC Press, 2004.

Kaza, S et al. What a waste 2.0: a global snapshot of solid waste management to 2050. World Bank Publications; 2018.

Kincaid, D.; Cheney, W. Numerical Analysis. Belmont, CA. Wadsworth, 1991.

Kuruneru, S.T.W. et al. Application of porous metal foam heat exchangers and the implications of particulate fouling for energy intensive industries. Rev. Chemical Engineering Science, Elsevier, v. 228, p.2, dec. 2020.

Magnanelli, E. et al. Dynamic modeling of municipal solid waste incineration. Rev. Energy, Elsevier, v. 209, p.1- 2, 2020.

Raja, B.D. et al. Multiobjective thermo-economic and thermodynamics optimization of a plate–fin heat exchanger. Heat Transfer, Wiley Online Library, v.47, p. 251-257, 2018. SAGE, A. P. Systems Engineering. John Wiley & Sons: New York, 1992.

Santos, M.L.S.; Ceribeli, K. Technical evaluation of a power generation process consuming municipal solid waste. Rev.Fuel, Elsevier, v. 108, p. 578–585, 2013.

Shapiro, B. Creating Compact Models of Complex Electronic Systems: An Overview and Suggested Use of Existing Model Reduction and Experimental System Identification Tools. IEEE Transactions on Components and Packaging Technologies. New York, v. 26, p. 165 – 172, 2003.

Trivelato, G. C. Técnicas de modelagem e simulação de sistemas dinâmicos. Ministério da Ciência e Tecnologia, Instituto Nacional de Pesquisas Espaciais – INPE, São José dos Campos, Brasil, 2003.

Vargas et al. A Numerical Model to Predict the Thermal and Psychrometric Response of Electronic Packages. Rev. Journal of Electronic Packaging, ASME, v. 123, p. 200–210, 2001.

Woods, R. L.; Lawrence, K. L. Modeling and Simulation of Dynamic Systems. Prentice-Hall, Upper Saddle River, New Jersey, 1997.